

First we would like to thank the reviewer for the second review which is full of ideas. They have been studied carefully but they have not been applied yet due to the framework which is not as free as we wish. In addition to the computational cost of particle modeling, we underline that the Meso-NH simulations have been performed for the BLLAST experiment and cannot be tuned at will.

Below is our response to the comments (in blue) on a point-by-point basis. The text referring to the article is indicated in italic.

Answers to major comments

1 Sub-grid turbulence model My previous comment was essentially that it appears that the model is inconsistent with behavior that is expected in a subgrid turbulence model. My claim was that the particles should be driven by the resolved Eulerian velocity field, and the Lagrangian model should be predicting the unresolved velocity.

Based on my understanding, the behavior of the model presented by the authors appears to be inconsistent with that of a subgrid-scale model. Perhaps this is because my understanding of the model formulation is still incomplete, in which case the authors may be able to explain its consistency through the following simple thought experiment. Simply consider how the model should respond as grid resolution is varied. As the grid scale approaches the Kolmogorov scale, the subgrid effects should tend toward zero (this is the most fundamental quality of a subgrid model). And in the context of the particle model, the particle velocity should match the Eulerian velocity : $V \rightarrow v$ and $W \rightarrow w$. Forgive me, but looking at the equation following Line 419 I don't see how this will happen. In the opinion of this reviewer, the authors either need to demonstrate that the model is at least consistent in this regard, or use a model formulation that is consistent.

I am still not entirely sure why the authors have set up their Lagrangian equations the way they have, rather than using a standard approach that is known to be consistent (it is no more difficult or costly). The authors are of course free to use any approach they like as long as it's consistent, I am just curious.

So why not calculate the total velocity V as the sum of the resolved Eulerian grid velocity (known, call it v) and model the unresolved component using the SLM (unknown, call it \tilde{v}); i.e., $V = v + \tilde{v}$? Note that in the current paper, $v = -\nabla_x p$ which is wrapped into the total equation for V , whereas here v is interpolated from the Eulerian simulation to the particle location and thus is 'known'. Then the evolution equation for v is left to model, which is

$$d\tilde{v} = -C_1 \frac{\varepsilon}{e} \tilde{v} dt + \sqrt{C_0 \varepsilon} dB \quad (1)$$

where ε and e are turbulent dissipation rate and subgrid TKE, respectively, which are interpolated from the Eulerian grid to the particle position. Now, our model will at least be consistent as the grid is refined : e tends toward zero as the grid scale tends toward zero (as a result this dissipation term becomes very large and damps out all fluctuations), and thus $\tilde{v} \rightarrow 0$ and $V \rightarrow v$. This formulation is also consistent if you go the other way and tend toward RANS. As the grid scale becomes very large, $e \rightarrow K$, $v \rightarrow \bar{v}$, $\tilde{v} \rightarrow v'$, and thus we converge to a standard RANS downscaling

model. This seems important for Meso-NH, which can be 'switched' between RANS and LES modes. Only in the case of RANS where no turbulence is resolved is the resolved velocity equal to $-\nabla_x p$ and the unresolved TKE equal to K .

An important point has to be clarified : the SLM aims at modeling the total wind speed using particles which sample the local wind pdf. The SLM has been designed regardless of the grid size of the model used to force it. Nevertheless the term "local" is related to the forcing scale. It can be understood as " a smaller scale than the forcing scale". Thus, if the forcing scale tends toward zero, the particles would sample the wind pdf into a very small of atmosphere. There is one limit : the SLM should be used to model wind and turbulence in the inertial sub-range.

The stochastic Lagrangian model that we used is consistent with the model described by Pope [6, 7]. The equation for the horizontal velocity V is as following :

$$V_{k+1} = V_k - \nabla_x \bar{p} \delta t - C_1 \frac{\varepsilon_k}{K_k} [V_k - \langle V \rangle] \delta t + \sqrt{C_0 \cdot \varepsilon_k} \Delta B_{k+1}^V$$

and the equation for the velocity increment is simply given by :

$$dV_{k+1} = -\nabla_x \bar{p} \delta t - C_1 \frac{\varepsilon_k}{K_k} [V_k - \langle V \rangle] \delta t + \sqrt{C_0 \cdot \varepsilon_k} \Delta B_{k+1}^V \quad (2)$$

where K_k is the turbulent kinetic energy and ε_k the dissipation rate. The average $\langle \cdot \rangle$ is computed using subsets of the particle system and a regularization function. The pressure gradient $-\nabla_x \bar{p} \delta t$ represents the increment of the averaged horizontal velocity. All these terms are also described by Pope in [6] for instance.

Using $V = v - \tilde{v}$, the terms of the equation 1 can be rearranged as following :

$$dV = dv - C_1 \frac{\varepsilon}{e} (V - v) dt + \sqrt{C_0 \cdot \varepsilon} dB \quad (3)$$

where dv is the increment of the horizontal Eulerian velocity, e the subgrid TKE and ε the dissipation rate. Thus there are two differences between the equations 2 and 3. The first one is the term chosen for the averaged velocity increment. We have chosen to use the pressure gradient to be consistent with the model described by Pope, whereas you suggest to use directly a velocity increment. In our work the model is coupled with a grid point model and the pressure gradient is computed using the grid point pressure field. If the grid scale approaches the Kolmogorov scale, there might be difficulties to compute a local pressure gradient. Thus in this case, our choice is not relevant, and the velocity increment should be used.

The second difference is about the TKE. In equation 2, the TKE K is the total TKE computed using the particle velocity. In equation 3, the sub-grid TKE e is used. This formulation is not consistent with the model of Pope which aims at modeling the total velocity. This is the main difference between the two equations.

To conclude, another choice can be done for the averaged velocity increment. A sentence will be added in the article to precise our choice. A quick test has been done by forcing the particle with the velocity increment. The results seem poorer (see figure 1).

Lines 445 of the authors' response : *The pressure gradient has be chosen to be consistent with the model described by Pope [7], but the mean horizontal velocity can be used instead in case of difficulty in computing the pressure gradient.*

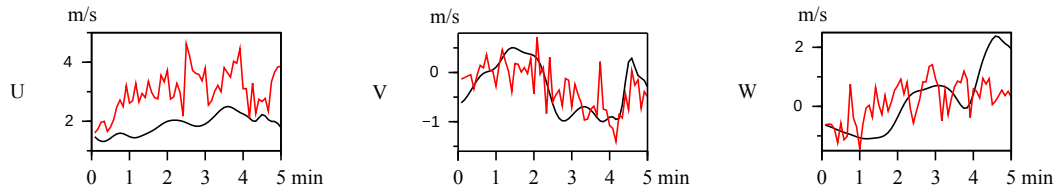


Fig. 1: Time evolution of the three wind components obtained from the fine Meso-NH simulation (black) and by the particle model (red) for one cell of the fine grid when the particle are forced directly by the velocity increment

2 Gaussian assumption Unfortunately, I am still in disagreement with the authors' position, as well as their newly added statements, e.g., "It leads that in this study, in a given grid cell, particles are samples of different Gaussian pdf." It doesn't matter if the turbulence statistics vary in space, the particle velocities will be locally Gaussian with variance, dissipation, etc. equal to the Eulerian value specified at that point. This is the idea behind the Pope/Thomson Lagrangian stochastic dispersion models. We specify a PDF at every point, and we seek to generate an ensemble of Lagrangian particles that has that PDF and has a local dissipation rate of ε . This is how the models are derived, and how they work out in practice. Any deviation from this is caused by numerical error (or in the authors' case it could be due to the arbitrary stochastic terms that were added). The advantage of using an SLM rather than just sampling a PDF is that the particle velocities are correlated in time (this is a result of the fact that they must have dissipation rate of ε , or more directly that they follow Kolmogorov's second similarity hypothesis). Also as a side note regarding why the histograms presented by the authors (Fig. 1 of reply) do not appear Gaussian: the sample size is too small to make such an assessment. With so few samples (i.e., 75), the histograms are unlikely to look Gaussian unless we get lucky. The authors can test this using the MATLAB code I provided in the previous review, and setting $N=75$. In this case the PDF will usually look quite non-Gaussian (depending on 'luck'), and as N is increased the PDF converges toward Gaussian.

With all that said, I am not particularly concerned with this issue as it pertains to the manuscript. The original motivation for this comment was related to the novelty of the paper. Let's say for the sake of argument that the authors are correct that for some reason the particle velocities are highly non-Gaussian when aggregated over a grid cell. Even if that is so, what is the novelty of the downscaling methodology when considering the work of, e.g., Bernardin et al. (2009)? Looking at their Eq. 19b, the only difference I see between the authors' velocity equation is the arbitrary "buoyancy" term that was added. Based on my own viewpoint, I would say that the novelty lies in the fact that the authors have used the Meso-NH model, which based on my limited understanding, is somewhat of a hybrid between a RANS and LES code. In that case, it seems that the downscaling method should be consistent in that regard, and thus it might make more sense to use the approach described in the previous comment.

As written in the previous answer the stochastic Lagrangian model (equations lines 419 of the author's response) describes actually a Gaussian pdf when it is applied to the whole particle system with the same forcing and when $\langle \cdot \rangle$ is the ensemble average over the particle system. However in our work, the forcing varies

in space and the average $\langle \cdot \rangle$ is computed for each particle using a different subset of the particle system and a regularization function. Thus a particle is driven by its own model and the particles are not identically distributed. In a grid cell, it leads to a mixing of local Gaussian models.

The buoyancy term in our Lagrangian model is not a significant term in this work. The buoyancy term indicates only that the model can be improved by modeling the temperature. In our work, it is simply modeled by a centered Gaussian variable with a very small variance.

There are several major differences between our method and the one described by Benardin in [3] :

- in [3] the forcing is done by giving boundary conditions for the particle velocities whereas in our work particles are forced by the pressure gradient and the dissipation rate in each cell,
- the boundary is "solid" in [3], that is to say that the particles rebound against the boundary, whereas we have chosen to let particles follow the air flow and to replace outgoing particles by new particles,
- Bernardin uses a $k - \varepsilon$ closure scheme for the dissipation rate whereas the dissipation rate is given by the grid-point model in our work,
- the way to compute the average $\langle \cdot \rangle$ differs : in our work it is computed using a Gaussian regularization function whereas in [3] it is the average of the particle velocities cell by cell – that is to say using a characteristic function. The advantage of our method is to take into account the continuity of the modeled atmosphere,
- the modeled scales are different : the horizontal grid size is 3km large in [3] whereas it is 40m in our work. Thus the application of these works are complementary but different.

3 Stochastic numerical error 'correction' term in the particle position equation

Can the authors provide any references that 'correct' for the numerical errors in this way? I can't see how adding additional dispersion somehow corrects for the numerical dispersion – in this case I don't see how two wrongs make a right, as both the error and correction appear to be additive and dispersive. Typically, numerical truncation errors are reduced by reducing the timestep, or there are refinement methods that use a systematic approach to (usually iteratively) improve the solution. Maybe the authors are using some method that I am unfamiliar with, in which case I am curious to read more (perhaps from a reference). Also, I would note that the 'correction' is being added to the position evolution equation, yet the explanation given by the authors seems to pertain to errors related to the velocity evolution equation. How are the two related?

The referee points out an interesting remark on the dispersive character of a noise added on the particle position. Let's back to the formulation.

The exact system is in continuous time without any noise added on the particle location. The Lagrangian particle velocity model is of McKean-Vlasov type and a Euler-Maruyama scheme is used. Some works of Bally and Talay (ex : [?]) give the shape of the integration errors for SDE. Then denoting V_{n-1} the velocity at time t_{n-1} , U_n the velocity at the time t_n given by the continuous integration starting

from V_{n-1} and V_n the approximated velocity given by the Euler integration scheme. Finally the Euler scheme error is denoted by v'_n and $U_n = V_n + v'_n$. v'_n is a random variable and the paper [2] gives information on its probability laws.

Concerning the integration of the particle locations, it yield with the same kind of notations, $X_{n+1} = X_n + \int_{t_{n-1}}^{t_n} U_s ds$. Then using the Euler approximated integration, the particle position is a random variable integrating the random variable v'_n along the path. This random path integration gives a random variable (see [5]). As suggested by the referee, it is possible to proceed to the approximation using small timesteps. But it always introduce an integration errors. Then to model this integration error, a random variable has been retained. Historically it comes from our works [1] on nonlinear filtering of velocity measurements on turbulent flows. Using the Bally and Talay work, using the shape of the particle Lagrangian model which is locally Gaussian, a Gaussian modeling seems to be suitable. There is an interesting discussion (section on particle mesh method and section on application) on this topic in the article of Pope [8]. Formally it is one of the reason that the discrete time nonlinear filtering problem solved by particle approximation do not collapse on a singularity.

In this work the limitation of the numerical costs has been privileged. Then the path errors due to the discrete time integration has been modeled by a Gaussian random variable. The variance of this Gaussian noise is limited to get a small random term with respect to the approximated velocity term. As remarked by the referee this choice of a random variable is dispersive. With a small number of particles, the dispersive effect isn't a drawback and allow to the particles to visit all the domain.

4 Rogue trajectories Overall, the authors' response was sufficient. I would recommend one thing the authors might try. What happens to the power spectra when you decrease the particle integration timestep δt by, say, an order of magnitude? Does it get rid of some of that extra energy at small-scales? If so, there may be some issues with numerical stability although it might not be manifesting as 'rogue' trajectories in the traditional sense.

It is an interesting idea, but decreasing the particle integration timestep by an order of magnitude increases the computational time by the same order. In view of our numerical framework, it is not possible to decrease the timestep without using another programming language.

5 Validation Even on the "fine" Meso-NH grid, the velocity field is presumably still missing unresolved (subgrid) energy, which I'm guessing is not negligible (looking at the spectra in Fig. 9, it appears to be substantial). This is why the Mesh-NH velocity is much "smoother" than the particle velocity. So the When you filter (i.e., average) to get the "coarse" grid, some additional energy is removed, let's call that Δe . So the total TKE for the coarse grid is $K_{res} + \Delta e + e$. Here is something to try : why not use Δe instead of e in Eq. 1 (above), and compare to the resolved TKE from the "fine" solution? In this case, the goal of the downscaling model is to

recover Δe rather than $\Delta e + e$, which means you can directly compare to K_{res} for the fine grid. My opinion is that simply saying that for future work "higher resolution simulations should be performed" is not acceptable.

Regarding a "toy problem" : I could think of some tests that could be useful here. What about generating some random 'turbulence' (could be white noise or correlated) on the "fine" grid, then filtering it to get a "coarse" grid? You could calculate the TKE of the fine grid turbulence (this is ' $K = K_{res} + e$ '), then calculate the TKE of the coarse grid (this is K_{res}). Now drive the particle model with e and downscale to the fine grid, where you should find that the TKE of the total particle velocity is K . This of course is non-physical and probably wouldn't go into the paper, but could be a good verification check to demonstrate consistency.

We underline that, in equation 2, K is the total TKE modeled by the particles. Using the subgrid TKE as suggested would not be consistent with the Lagrangian model described by Pope.

The idea behind the sentence "higher resolution simulations should be performed" is to perform grid point simulations with a finer grid size without changing the forcing scale. Thus the idea is to compare the particle fields that we already have to grid point simulations using a grid finer than 40m x 40m x 12m. Unfortunately, it has not been possible to perform such simulations with Meso-NH for this work.

The suggested test does not seem suitable with our forcing method. The subgrid TKE is not used to force the particle system. Indeed, we use the total particle TKE in the Lagrangian model and the pressure gradient and the dissipation rate are used to force the particle system. Forcing the particle system by the TKE requires a new formulation of the model. Thus we have not adapted the test to our work, but it might be done in further works.

Answer to minor comments :

1. In my own experience, the term 'downscaling' is usually used to describe a one-way model from large to small scales, whereas 'sub-grid modeling' is typically reserved for two-way coupling where the large-scale model needs to parameterize the small-scales. I would consider this work to address downscaling. I would leave it up to the authors discretion, but they may consider revising the title and certain other instances to make this point clear.

Thank you for the suggestion. It has been changed in the manuscript.

2. Line 25 : model \rightarrow models

The correction has been made.

3. Lines 41-44 : Consider re-wording this sentence. How can AROME airport resolve processes? The authors probably mean that processes at the scale of AROME airport are not resolved.

The correction has been made.

4. Lines 80-86 : The first statement seems to say that an assumption is made that the local PDF is Gaussian. Then it says that locally the PDF samples multiple Gaussian PDFs, and therefore it is not necessarily Gaussian. These seem to contract each other.

We suggest to add a sentence to clarify this point. Line 70 of the previously

revised manuscript / line 80-86 of the authors' response : *The method we suggest differs from these previous works : the Gaussian assumption on the pdf shape is only locally made. This locally Gaussian assumption is linked to the use of a local average operator presented in section 3.6. As explained in this section, in this study the locally Gaussian assumption is not equivalent to have a Gaussian pdf in each cell. It leads that in a given grid cell, particles are samples of different Gaussian pdf. Therefore they give access to a discrete pdf which is not necessarily Gaussian.*

5. Sect. 3.2 : What is meant by the term 'coupling experience'? In English, this phrase sounds a bit unusual. Is there some particular reason to use the word 'experience', rather than just saying something like 'model coupling', or 'coupling between resolved and unresolved scales'?

The correction has been made.

6. Sect. 3.3 : Consider moving this section until after the model has been introduced (i.e., beginning of Sect. 6). Currently, it feels out of place since this is really just details related to model testing/validation and is not central to the model itself.

The section 3.3 has been moved in section 4.

7. 400-403 : Can the authors explain why they feel that the ideas presented by Kolmogorov are considered "laws"? Typically these ideas are referred to as 'Kolmogorov theory' or 'Kolmogorov's hypothesis', as they are largely based on similarity/scaling arguments.

In French, the word "laws" is used. It has been replaced by "theory" in the manuscript.

8. 400-403 : How exactly is the model consistent with Kolmogorov theory? Would the authors consider it to be consistent with all of the similarity hypotheses presented in K41, or is it that it is consistent with Kolmogorov's second similarity hypothesis in that the variance of the Lagrangian velocity increments ($\langle du^2 \rangle$) is proportional to the turbulence dissipation rate, i.e., $C_0 \varepsilon dt$?

As explain by Pope in [6, 7], the model is consistent with Kolmogorov's second similarity hypothesis. This point has been added to the manuscript.

9. Lines 419.5 (equation) : I am not entirely clear on how K is specified. Normally, this would come from the large-scale simulation and be interpolated to the particle position. On Lines 308-310, the authors mention that the TKE is extracted from Meso-NH, which would lead me to believe that is where K comes from. However, Sect. 5.2 would suggest otherwise, that somehow the TKE is calculated afterward, although it is required in the velocity equation itself. Please explain.

As it is explained lines 447-451 of the authors' response, the term K in the SLM equations does not come from the model Meso-NH. This variable represents the total TKE and it is not used to force the particle system. It is computed using the particle velocities and a local average operator. This kind of average operator is also used by Pope in [7].

10. Lines 423-426 : The statement regarding the buoyancy term is vague. There are an infinite number of ways in which this term could be modeled using a random variable. Was this simply an empirical 'knob' that was turned?

The buoyancy is modeled by a centered Gaussian variable with a small variance

of $0.05 \text{ m}^2/\text{s}^2$. The variance value has been set to a small value on purpose. Indeed the buoyancy term is in the model only to show the possibility to improve it by modeling the temperature.

11. Lines 504-505 : How is the particle velocity initialized ? This seems important considering that the particle simulation times (Δt) are much shorter than the integral time scale, and therefore they are likely to 'remember' the initial condition.

There is an error lines 504-505 of the authors' response. The particle velocities are initialized using the velocities of the coarse Meso-NH simulation. The correction has been made in the manuscript.

12. Sect 3.6 : This title seems inappropriate. When are structure functions ever calculated in the paper ? It seems like a more appropriate title might be 'Ensemble averaging' or something of that nature.

The title of section 3.6 has been changed as suggested.

13. Lines 635-651 and Figure 7 : I don't see the value of this comparison. Firstly, the simulations and the data are not over the same time period. Secondly, am I supposed to look at Fig. 6 and Fig. 7 and say "Yes, the Meso-NH velocity is smoother than the sonic data" ? It would be incredibly surprising if that were not the case considering that the simulations don't resolve below the grid scale. In agreement with the comment, the figure 7 has been removed. A reference to [?] has been added.

14. Lines 671-674 : Should we not expect better agreement if the method is consistent ?

We continue to find that the results are in good agreement with the fine Meso-NH simulations, especially for the horizontal wind. It leads us to think that the forcing method works but the Lagrangian model may be improved for the vertical velocity. The following lines have been added (line 668) : *However one can notice that the results are better for the horizontal wind components than for the vertical one. To improve this point, one way could be to supplement the SLM with an equation for the temperature in order to model the buoyancy effect.*

15. Lines 855-858 and Fig. 12 caption : It is not clear to me how exactly the 'new' grid was obtained. If the grid resolution is changed, shouldn't the 'Meso-NH' TKE (black line) change as well ?

The new coarse grid is obtained by averaging the fine grid by groups of $2 \times 2 \times 2$ cells instead of $4 \times 4 \times 2$ cells for the previous coarse grid. Thus the new grid size is $40 \text{m} \times 40 \text{m} \times 24 \text{m}$. In the figure showing the different TKE (figure 12 of the first authors' response), the black line represents the TKE of the fine Meso-NH simulations. The resolution of these simulations does not vary in our work. The following clarification for the new coarse grid has been added line 857 : *This new grid is obtained by averaging the fine grid on $2 \times 2 \times 2$ cells.*

16. Sect. 6.1.3 (velocity spectra) : I have quite a few concerns with this section :
 - For the SLM used here, we know that 1. An ensemble of particles at any location should have TKE K , and 2. The variance of particle velocity increments at any location should be $\langle du^2 \rangle = C_0 \varepsilon dt$, which is consistent with Kolmogorov theory. Given this, should we expect the particle velocity spectra to follow $k^{5/3}$ scaling ?

The SLM has been designed to follow the $k^{-5/3}$ scaling [6]. Here the idea is to assess the behaviour of particles driven by the SLM when it is forced by Meso-NH –that is to say when the pressure gradient and the dissipation rate are given by Meso-NH.

- How the information presented in this section considered 'validation'?

As the modeled scales are in the inertial subrange, the wind spectra are expected to follow the $k^{-5/3}$ scaling. This section aims at ensuring that the particle wind spectra follow the scaling.

- This section appears to be missing a description of how the velocity spectra are calculated using the Lagrangian particle data.

First the particle velocities are averaged fine grid cell by fine grid cell in order to get a grid point field for the particle velocity. Then the particle velocity spectra are calculated using the same method than for the Meso-NH velocity spectra. The explanation is given lines 692-697 of the previous authors' response.

- Is the statement on Lines 717-718 meant to imply that the averaging time is insufficient? If so, why present these results?

These results show clearly that the particle wind spectra present regular slopes. This is a good point to assess the use of the stochastic downscaling method. The SLM is also used for turbulence estimation [9], and in this context, the spectra are computed using longer data sets – about 1h of data with a 4 second time step. This is why we think that longer simulations are needed to fully validate the model behaviour.

Références

- [1] C. Baehr. Nonlinear filtering for observations on a random vector field along a random path. application to atmospheric turbulent velocities. *ESAIM : Mathematical Modelling and Numerical Analysis*, 44(05) :921–945, 2010.
- [2] Vlad Bally and Denis Talay. The law of the euler scheme for stochastic differential equations. *Probability theory and related fields*, 104(1) :43–60, 1996.
- [3] Frédéric Bernardin, Mireille Bossy, Claire Chauvin, Philippe Drobinski, Antoine Rousseau, and Tamara Salameh. Stochastic downscaling method : application to wind refinement. *Stochastic Environmental Research and Risk Assessment*, 23(6) :851–859, 2009.
- [4] Guylaine Canut, Fleur Couvreur, Marie Lothon, Dominique Legain, and Bruno Piguet. Turbulence measurements with a tethered balloon. *Submitted to Atmospheric Chemistry and Physics*, 2016.
- [5] K Ito and H P McKean Jr. Diffusion processes and their sample paths, 1965.
- [6] SB Pope. Lagrangian pdf methods for turbulent flows. *Annual review of fluid mechanics*, 26(1) :23–63, 1994.
- [7] Stephen B Pope. *Turbulent flows*. Cambridge university press, 2000.
- [8] Stephen B Pope. Simple models of turbulent flows a. *Physics of Fluids*, 23(1) :011301, 2011.

- [9] Lucie Rottner and Christophe Baehr. Real time turbulence estimation using doppler lidar measurements. In *EPJ Web of Conferences*, volume 119, page 14001. EDP Sciences, 2016.

A new downscaling method for sub-grid turbulence modeling

L. Rottner¹, C. Baehr¹, F. Couvreur¹, G. Canut¹, and T. Rieutord¹

¹Météo-France - CNRS, CNRM / GAME, UMR 3589, 42 avenue Coriolis, 31100 Toulouse

Correspondence to: Lucie Rottner (lucie.rottner@meteo.fr)

Abstract.

In this study we explore a new way to model sub-grid turbulence using particle systems. The ability of particle systems to model small scale turbulence is evaluated using high resolution numerical simulations. These high-resolution simulations have been performed with the research atmospheric model Meso-NH and averaged at larger scale from which a complete downscaling experience, via a particle system, have been performed. The particle simulations are compared to the high-resolution simulation for the representation of the wind fluctuations and the turbulent kinetic energy. Despite the simplicity of the physical model used to drive the particles, the results show that particle system is able to represent the average field. It is shown that this system is able to reproduce much finer turbulent structures than the numerical high-resolution simulations. In addition, this study provides an estimate of the effective spatial and temporal resolution of the numerical models. This highlights the need for higher resolution simulations to be able to evaluate the very fine turbulent structures predicted by the particle systems. Eventually a study of the influence of the forcing scale on the particle system is presented.

1 Introduction

Following the increase in computing power, the resolutions of meteorological ~~model~~ models have increased steadily over the past years. The refinement of the temporal and spatial resolution of atmospheric model requires a finer and finer representation of physical phenomena. The current weather forecast models have a kilometric resolution. However, the small processes, which have local effects, are still sub-grid processes in such models. Thus they are subject to physical parametrization.

The ~~sub-grid modeling~~ downscaling issue concerns many meteorological research fields, from snow pack modeling to cloud cover modeling. A particularly delicate matter is to

model the turbulence in the Atmospheric Boundary Layer (ABL). In the ABL there is a transfer of energy from kilometric scales to metric scales. This transfer is called the energy cascade. Thus whatever the model resolution, some turbulent processes are sub-grid processes. For numerical weather forecast models, the processes associated to kilometric scales are not resolved yet. For instance, a recent study shows that these processes are not resolved ~~by~~ at the scale of AROME Airport which has a horizontal resolution of 500 meters (Hagelin et al., 2014). As the local turbulence is a pilot of the local atmosphere evolution, for high resolution modeling a key point is to use a good turbulence parametrization. For instance, recent studies have shown the influence of the turbulence parametrization on the cloud modeling in tropical regions (Machado and Chaboureau, 2014). Several field experiments have helped to understand the influence of small scale turbulence on local weather conditions – the erosion of the nocturnal valley inversion for instance (Rotach et al., 2004; Drobinski et al., 2007; Rotach et al., 2008).

Because of their variability and their sensitivity to local conditions, these turbulent phenomena are especially difficult to model. Instead of a larger decrease of the grid size, we suggest here another way to model sub-grid turbulence. In this paper, we present a stochastic downscaling approach. Our method is based on particle systems that are driven by a local turbulence model. Those particles are embedded in grid cells (illustration 1). From the mathematical point of view, the particles sample the probability density function (pdf) of the sub-grid wind. The description of sub-grid processes based on their pdf has been introduced by Sommeria and Deardorff since 1977 (Sommeria and Deardorff, 1977). The Gaussian approximation they made to describe the liquid water content has then been extended to other variables. Nowadays, this kind of approximation is still widely used for ~~sub-grid modeling~~ downscaling (Larson et al., 2002; Perraud et al., 2011; Larson et al., 2012; Jam et al., 2013; Bogenschütz and Krueger, 2013). The method we suggest differs from these previous works : the Gaussian assumption

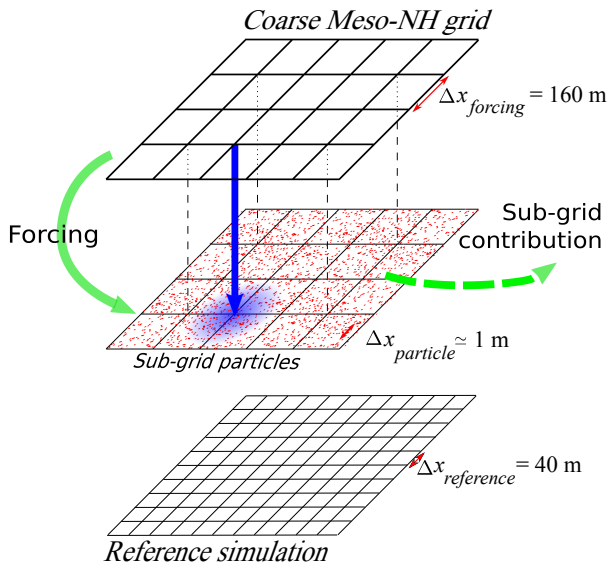


Figure 1. The downscaling experience. Coarse fields are used to force a sub-grid particle system. The sub-grid fields are compared to a reference Meso-NH simulation.

on the pdf shape is only locally made. This locally Gaussian assumption is linked to the use of a local average operator presented in section 3.5. [As explained in this section, in this study the locally Gaussian assumption is not equivalent to have a Gaussian pdf in each cell.](#) It leads that in [this study, in](#) a given grid cell, particles are samples of different Gaussian pdf. Therefore they give access to a discrete pdf which is not necessarily Gaussian. The pdf time evolution is thus given by the particle evolution. The suggested particle approach enables to model physical phenomena with nonlinear temporal evolutions. However, depending on the particle model, particle methods may have drawbacks such as interpolation issues for instance Brackbill et al. (1988). In the present work, the only delicate point is to ensure that the particle density is high enough in each grid cell.

In order to keep the average particles behavior consistent with the grid-point model, some grid-point fields are used as an external forcing on the particle system. The grid-point fields provide the values of the control parameters of the particle evolution model. This forcing is constant during the grid-point model time step and is applied every time new values are available. However, the particle evolution is performed at a shorter time step. Thus, the suggested downscaling method enables to refine both time and space scales.

In this work, the French research model Meso-NH is used to obtain high resolution grid-point fields. The chosen simulations have been performed for the BLLAST experiment (Lothon et al., 2014). Therefore we have used simulations and observations of real turbulent ABL to develop a stochastic downscaling method suitable for limited area model.

First the framework is presented. The BLLAST field experiment and the experience of particle system and grid-point model coupling are introduced. A description of the models follows in the section 3. Then section 4.2 details the forcing procedure. A brief presentation of the turbulent kinetic energy computation is given in section 5. The results obtained using the suggested downscaling method are then presented. We finally discuss their sensitivity to the resolution of the forcing fields in section 7.

2 The BLLAST experiment

The BLLAST (Boundary Layer Late Afternoon and Sunset Turbulence) field campaign was conducted from 14 June to 8 July 2011 in southern France, in an area of complex and heterogeneous terrain. The BLLAST experiment resulted from a collaboration of several European laboratories spearheaded by the Laboratoire d'Aérologie. The experiment aim is to study the turbulence in the boundary layer during the late afternoon transition (Lothon et al., 2014).

To perform this study, all turbulence sources were investigated. A wide range of integrated instrument platforms including full-size aircraft, remotely piloted aircraft systems (RPAS), remote sensing instruments, radiosoundings, tethered balloons, surface flux stations, and various meteorological towers were deployed over different surface types (Pardyjak et al., 2011). In addition to the numerous observations, high resolution simulations of the boundary layer have been done using Large Eddy Simulation (LES) models. Then the model ability to simulate turbulence has been evaluated (Jimenez et al., 2014).

The BLLAST experiment addresses a wide range of scientific issues such as the turbulence decrease (Darbieu et al., 2015), the wind direction variability, or the turbulent kinetic energy budget (Nilsson et al., 2016). The diversity of the available observations and simulations, and the dynamism of the BLLAST community lead us to choose this experiment to develop the presented downscaling method.

3 Models

Now that the BLLAST experiment has been presented, let us introduce the two models used in this work. First the grid point model is presented, and the coupling experience is described. Then the focus is put on the particle system and its evolution model.

3.1 Grid-point model Meso-NH

To perform the grid-point simulation of the ABL, we have used the research model Meso-NH. It is a non-hydrostatic mesoscale atmospheric model jointly developed by the Laboratoire d'Aérologie and by CNRM-GAME (Lafore et al., 1998). It incorporates a non-hydrostatic system of equations,

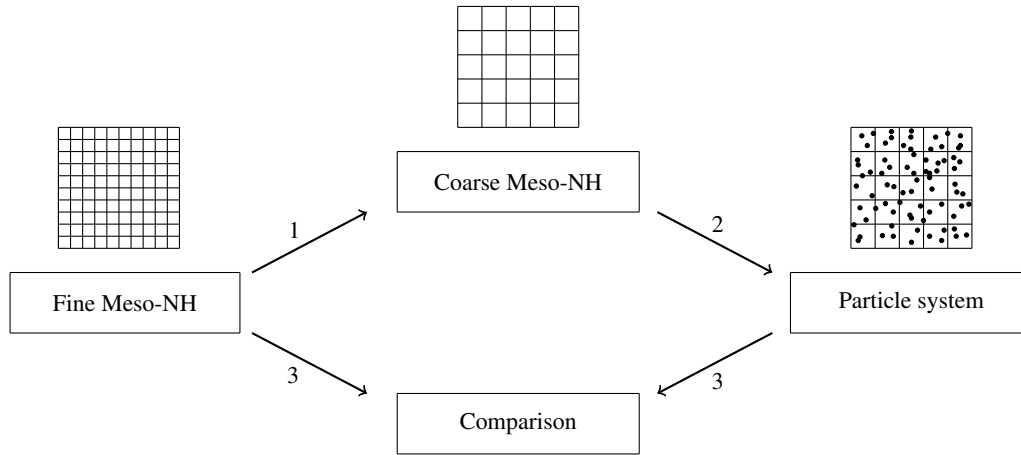


Figure 2. Our study framework. We use a fine model, which is degraded to get a coarse one. Particles are forced with coarse fields. Then we compare fine fields to particle fields.

and deals from large (synoptic) to small (large eddy) scales. Meso-NH has a complete set of physical parametrizations for sub-grid modeling. The Meso-NH model is thus a reference tool to model turbulence. It has already been used to evaluate the quality of the turbulence representation in models at kilometeric scale (Honnert et al., 2011). Furthermore, Meso-NH can be used in a LES mode (Couvreux et al., 2005). Then its high effective resolution enables to model the main turbulent processes.

The equation system resolved by the Meso-NH model is an approximated form of the Durran (1989) version of the anelastic system. Meso-NH is an Eulerian model which uses a fourth-order centered advection scheme for the momentum components and a finite-volume method for advection of meteorological variables (e.g. temperature, water species, turbulent kinetic energy) and passive scalars (Colella and Woodward, 1984). In order to suppress the very short wavelength modes, the model uses a fourth-order diffusion scheme applied only to the fluctuations of the wind variables.

For our simulations, the 3D turbulence scheme is a one and a half order closure scheme (Cuxart et al., 2000). Thus the sub-grid TKE is a prognostic variable whereas the mixing length is a diagnostic variable. The mixing length and the dissipative length are computed separately according to Redelsperger et al. (2001). The mixing length is given by the mesh size depending on the model dimensionality. This length is limited to the ground distance and also by the Sommeria and Deardorff (1977) mixing length, which is pertinent in the stable cases. The eddy dissipation rate is computed from the subgrid turbulent kinetic energy using a closure scheme based on the mixing length.

3.2 The Model coupling experience

To introduce the presentation of the Meso-NH simulation which has been used, the framework of the coupling experience is now described.

Our experience is a first step in coupling particle systems and grid-point models. Here, we work on the downscaling from the grid-point model to the particle system in one way, so the information flow goes only from the grid-point model to the particles. We have used simulations of convective boundary layer to force a particle system which models sub-grid turbulent phenomena.

The particle systems are forced with a large scale grid-point meteorological fields. The large scale used in our work is later described in details. The forced particles are used to model the sub-grid fields for the large scale model. To validate the sub-grid modeling downscaling a higher resolution model is used. In theory, the turbulent fields represented by the particles should be compared to the same fields simulated by a high resolution grid-point simulation. For computational reasons we do not have access to different high resolution simulations. Thus the large scale simulations have been built from the available simulations.

The process consists of three steps as outlined in figure 2. First, we have performed high resolution simulations with the model Meso-NH. These simulations are the finest available simulations. So they are considered as a reference and represent the real atmosphere. The high-resolution simulations are not directly used to force the particles. Thus, they can be used to independently assess the turbulence modeled by the particle system.

Now that we have a reference simulation, a coarser simulation is built in order to force the particle system. To this end, we have chosen to average the grid-point fields on few cells. To be consistent, we have also applied a temporal average. The obtained coarse Meso-NH fields have thus lower spa-

tial and temporal resolutions than the reference simulation while being consistent with it. However, due to the average, the coarse fields include not only the components resolved on the grid, but also the average of the sub-grid components. This limitation will be discussed in section 8.

In each cell of the coarse grid and during each coarse time step, the particle average behavior is forced. If the forcing method works, the average of the particles should be in good agreement with the coarse fields.

To assess the method, we have worked on wind fields and turbulent kinetic energy (TKE) fields. As explained in section 4.2, the TKE and the horizontal wind are not directly forced by the coarse model. The models and the data we used are presented in the two following sections.

3.3 Meso-NH simulation

~~The domain of simulation : 8x8x4 fine cells which are grouped in 2x2x2 coarse cells.~~

~~As Meso-NH is a research model, its grid size and its time step may differ from one simulation to another. For the simulation used here, the horizontal grid size is $\Delta_x = 40\text{m}$, and the vertical one is $\Delta_z = 12\text{m}$. This simulation uses the set-up of Darbieu et al. (2015), and uses a 256x256x256 points domain with cyclic conditions. The simulation starts at 06h00 and lasts 15 hours. Because of the high computational time of the simulations, we present here only 15 minutes of simulation with a $\delta_t = 5\text{s}$ time step. Moreover, to avoid the explosion of the computational time of the forcing procedure, we have only kept a 8x8x4 grid points. The first vertical level altitude is around 360 meters. The data are chosen in the middle of the ABL for two reasons. First, at these heights, issues linked to the vicinity of the ground are avoided. In addition, in convective conditions, the turbulence is well established in the middle of the ABL. In the following sections, this configuration of Meso-NH is called the fine reference configuration. It will be used to evaluate the fields reconstructed with the particle system.~~

~~To force the particles, averaged fields are used. They are deduced from the reference fields. The averaged fields, called coarse fields, are obtained by averaging several grid points, on 12 time steps ($\Delta_t = 1\text{min}$). Each average is made on a 4x4x2 grid points domain (figure 3). So, the coarse grid size is 160mx160mx24m.~~

~~We have selected data from 13h55 to 14h10 during the convective period, the 06/20/2011. Among all the available variables in Meso-NH, we have extracted the atmospheric pressure, the 3 components of the wind, the TKE and the eddy dissipation rate (EDR), for the reference configuration. The pressure gradient is computed using the pressure field. The previously described average has been applied to these reference fields to obtain the coarse fields. We underline that only the coarse fields are used to force the particle system. The reference fields are simply used to evaluate the fields obtained from the particles.~~

~~To ensure its consistency with the real case, the high resolution Meso-NH simulation has been compared to another LES simulation performed with the LES model of the National Center for Atmospheric Research (NCAR) for the same case and shows similar results (Darbieu et al., 2012).~~

3.3 The particle system

In order to model the sub-grid processes, an applied mathematical technique is used : the probability density functions are described using a particle system. In this study, the particles sample the wind probability density function. The particle technique is widespread in research fields such as mechanical system modeling (automotive, aeronautics), but it is not yet currently used for atmospheric modeling. However, Lagrangian particle models for dispersion have been discussed for quite a long time. Guidelines to evaluate the relevance of a stochastic model have been given by Thomson (1987), and different particle pair models for dispersion and concentration fluctuations are described in Thomson (1990) and Durbin (1980). These models have then been improved and generalized to particle system models for dispersion and air pollution modeling (Uliasz, 1994; Stohl and Thomson, 1999).

Here, a particle is a realization of the surrounding atmosphere. Depending on the complexity of the evolution model, the particles carry physical properties, such as fluid velocity, temperature or humidity rate. In our study, the evolution model is simple, and each particle is a position/velocity couple. Using the particle approximation of the probability density function and the physical properties of the particles, the statistics of the turbulence are computed. In particular, the wind variance can be computed. Thus using the particle wind, the TKE is directly available.

The suggested stochastic downscaling method completes the long list of downscaling techniques developed to improve geophysical model resolutions. Among them, we find the adaptive mesh refinement for oceanic and atmospheric models (Blayo and Debreu, 1999; Debreu et al., 2005; Andrews, 2012). Our downscaling method offers an other point of view. Instead of refining the grid, the sub-grid atmosphere is modeled using a particle system which lives inside the grid cells.

Previous studies have already explored stochastic downscaling methods for the meteorological model MM5 (see Rousseau et al. (2007), Bernardin et al. (2009), and Bernardin et al. (2010)). As these studies, our work aims at modeling the wind at very small scales on a limited area. The same particle evolution model is used. In these studies, the downscaling is performed by imposing the boundary conditions. The conditions are given by a large scale Eulerian model. It ensures the consistency of the particle system with the large scale model. Moreover, it enables to keep particles

inside the simulation domain. Indeed, the forcing induces a reflection of the particles against boundary.

325 Different choices have been made to develop the presented downscaling method. We have chosen to force the particles cell by cell using the grid-point fields, but there is no imposed condition to the edge of the domain. The particles live freely in the domain and may go from one cell to another. 330 When some particles go out the domain, they are deleted and replaced by new particles inside the domain. For each new particle, the particle position is randomly chosen. Then the new particle velocity is computed using the velocities of the particles which are in the same cell. Thus the particle system contains information relative to different scales, including local components of the fields associated to sub-grid scale and large or mean components coming from the forcing, associated to the grid scale. 375

To compare the fields represented by the particles to the grid-point fields modeled with Meso-NH, an average on the particle values is made cell by cell. For instance, the wind \mathbf{V}_α represented by the particles in the cell α is given by the following expectation : 380

$$\mathbf{V}_\alpha = \frac{1}{N} \sum_{i=1}^N \mathbf{V}_\alpha^i$$

where N is the number of particles in the cell α , and \mathbf{V}_α^i 385 is the velocity of the particle i . If the sub-grid processes are rightly modeled by the particle system, the fields represented by the particles should be similar to the fine Meso-NH fields. The results of the [sub-grid modeling downscaling](#) are presented section 6. They are obtained with 75 particles in each fine grid cell. Thus the whole system contains 19200 particles. This number may be compared to the 800 particles per grid cell used by Bernardin et al. (2009) for the same kind of application. 395

3.4 The Stochastic Lagrangian Model

350 For the particles to be realizations of the surrounding atmosphere, the particle evolution is driven by a local turbulence model. It is a Stochastic Lagrangian Model (SLM) inspired from Pope (2000) and introduced for atmospheric turbulence estimation purpose by Baehr (2009, 2010). The model is consistent with [the Kolmogorov laws - Kolmogorov's similarity hypothesis](#) for turbulence (Kolmogorov, 1941). It describes the evolution of the position, X , and the 3D velocity of each particle. The position evolution is done by integrating the velocity. The velocity is split in one term for the horizontal velocity, V , and an other for the vertical velocity, W . Their evolutions depend on the local properties of the atmosphere and also on the atmospheric large scale characteristics. 410

In the evolution equations, the large scale influence is given by the pressure gradient $\nabla_x \bar{p}$ for the horizontal velocity, and by the mean vertical velocity increment $\Delta_k W$ for the vertical velocity. The velocity evolution depends on the local

properties through a term of wind fluctuation around the locally averaged wind, $\langle V \rangle$ and $\langle W \rangle$. The local average operator $\langle \cdot \rangle$ is described in the next section. Then, for the vertical velocity, the buoyancy effect is taken into account. The last term of the equations is a dispersion term. It is represented by a Wiener process ΔB^\bullet normalized by the time step δt . Finally, the SLM equations are given by :

$$\begin{cases} X_{k+1} = X_k + \mathbf{V}_k \delta t + \sigma^X \Delta B_{k+1}^X \\ V_{k+1} = V_k - \nabla_x \bar{p} \delta t - C_1 \frac{\varepsilon_k}{K_k} [V_k - \langle V \rangle] \delta t \\ \quad + \sqrt{C_0 \cdot \varepsilon_k} \Delta B_{k+1}^V \\ W_{k+1} = W_k + \Delta_k W - C_1 \frac{\varepsilon_k}{K_k} [W_k - \langle W \rangle] \delta t \\ \quad + \frac{g}{\beta} \Gamma_k^\theta \delta t + \sqrt{C_0 \cdot \varepsilon_k} \Delta B_{k+1}^W \end{cases}$$

where g is the standard gravity, ε_k is the EDR and K_k the TKE. C_0 is the constant of Kolmogorov. The constant C_1 is given by $C_1 = \frac{1}{2} + \frac{3}{4} C_0$ as Pope suggested it (Pope, 1994).

The buoyancy effect term $\frac{g}{\beta} \Gamma_k^\theta$ is not directly modeled here. It is replaced by a random variable. We have chosen to use a centered Gaussian variable. This choice has been done for a sake of simplicity. However an equation for the temperature evolution may be added to improve the buoyancy effect modeling. One can notice the noise term at the end of the position evolution equation. The added term in the particle location has been included to take into account the velocity integration errors considering the Euler scheme used for the velocity equation (see Bally and Talay (1996)).

The stochastic Lagrangian model has two control parameters for the velocity equation. The EDR, ε , and pressure gradient, $\nabla_x \bar{p}$, are the control parameters for the horizontal velocity. For the vertical velocity, they are the EDR ε and the velocity increment $\Delta_k W$. In our downscaling method, they are given by the Meso-NH coarse simulation : it is how the coarse model forces the particle system. The two control parameters are related to the different scales modeled in the Meso-NH simulation. The pressure gradient and the vertical velocity increment are related to large scales, whereas the EDR is related to small scales. Thus each parameter is associated to an extremity of the energy cascade described by Kolmogorov. [We The pressure gradient has be chosen to be consistent with the model described by Pope \(2000\), but the mean horizontal velocity can be used instead in case of difficulty in computing the pressure gradient. We also underline that the EDR used to force the system is a diagnostic variable of Meso-NH. Therefore, it is computed using a closure scheme. This choice is discussed in section 8. Contrary to the EDR, the TKE, noted \$K\$ in the equations, does not come from the Meso-NH simulation. Instead we use the TKE computed using the particle system and the local average operator described in the next section.](#)

3.5 [Structure function computation Ensemble averaging](#)

As we have seen, the SLM equations contain some locally averaged terms, denoted by $\langle \cdot \rangle$. In our framework, the

fields are represented by the particle system. Thus only discrete representations on irregularly spaced points of the fields are available. It leads to a tricky implementation of the average. A regularization function G^δ is introduced. To compute the average at a point x , this function gives a weight to the particles depending on their distance to x . Then the local average is the weighted average of the particle values. The regularization function G^δ is a Gaussian which is centered at the computation point x . The variance of the function is noted δ^2 . The standard deviation δ is a length which depends on the homogeneity of the medium. Therefore, if the medium is homogeneous, the average can be computed using all the particles. In this simple case, the length δ can be long. On the contrary, if the medium presents strong spatial variations, only very close points have to be taken in account to get a representative average. Then the length δ has to be short.

To validate the downscaling method, the particle fields are compared to the fine Meso-NH simulation. In a grid-point model, the characteristic length of the modeled processes is twice larger than the grid size according to the Nyquist's frequency (Nyquist, 1924, 1928). Thus the grid size may be seen as the characteristic length, and we set the length δ at the finest Meso-NH grid size. As the horizontal grid and the vertical grid have different sizes, the horizontal characteristic length is set at $\delta_h = 40\text{m}$ and the vertical one is set at $\delta_v = 12\text{m}$.

The average operator $\langle \cdot \rangle$ is used to compute any needed structure functions. In particular the velocity variance may be computed using the local average and the particle system. The TKE is thus available at each time step. The **structure function-ensemble averaging** computation is independent of the forcing model grid. The particle system is viewed as a whole, and the local average may be computed using particles which are in different cells.

To compare the particle TKE to the TKE simulated by Meso-NH, the particle values are averaged cell by cell as explained in section 3.3.

4 The particle-system forcing

4.1 Meso-NH simulation

As Meso-NH is a research model, its grid size and its time step may differ from one simulation to an other. For the simulation used here, the horizontal grid size is $\Delta_x = 40\text{m}$, and the vertical one is $\Delta_z = 12\text{m}$. This simulation uses the set up of Darbieu et al. (2015), and uses a $256 \times 256 \times 256$ points domain with cyclic conditions. The simulation starts at 06h00 and lasts 15 hours. Because of the high computational time of the simulations, we present here only 15 minutes of simulation with a $\delta_t = 5\text{s}$ time step. Moreover, to avoid the explosion of the computational time of the forcing procedure, we have only kept a $8 \times 8 \times 4$ grid points. The first vertical level altitude is around 360 meters. The data are chosen in the

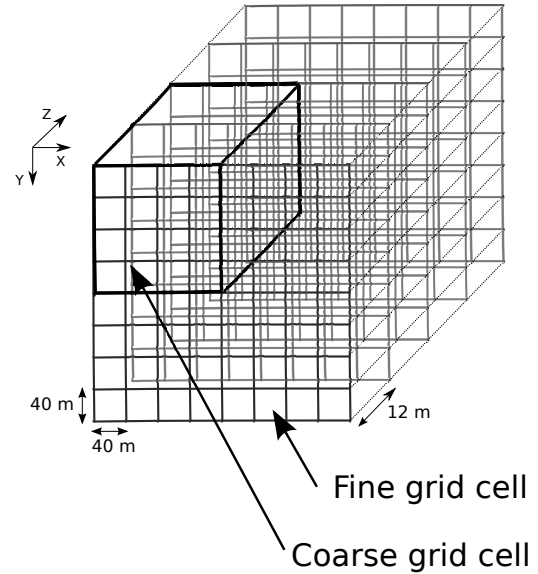


Figure 3. The domain of simulation : $8 \times 8 \times 4$ fine cells which are grouped in $2 \times 2 \times 2$ coarse cells.

middle of the ABL for two reasons. First, at these heights, issues linked to the vicinity of the ground are avoided. In addition, in convective conditions, the turbulence is well established in the middle of the ABL. In the following sections, this configuration of Meso-NH is called the fine reference configuration. It will be used to evaluate the fields reconstructed with the particle system.

To force the particles, averaged fields are used. They are deduced from the reference fields. The averaged fields, called coarse fields, are obtained by averaging several grid points, on 12 time steps ($\Delta_t = 1\text{min}$). Each average is made on a $4 \times 4 \times 2$ grid-points domain (figure 3). So, the coarse grid size is $160 \times 160 \times 24\text{m}$.

We have selected data from 13h55 to 14h10 during the convective period, the 06/20/2011. Among all the available variables in Meso-NH, we have extracted the atmospheric pressure, the 3 components of the wind, the TKE and the eddy dissipation rate (EDR), for the reference configuration. The pressure gradient is computed using the pressure field. The previously described average has been applied to these reference fields to obtain the coarse fields. We underline that only the coarse fields are used to force the particle system. The reference fields are simply used to evaluate the fields obtained from the particles.

To ensure its consistency with the real case, the high resolution Meso-NH simulation has been compared to another LES simulation performed with the LES model of the National Center for Atmospheric Research (NCAR) for the same case and shows similar results (Darbieu et al., 2012).

4.2 The particle system forcing

The aim of this work is to study the ability of a particle system forced by grid-point data to model the sub-grid processes. To do so, we use two grid-point simulations : a coarse one to force the particle system and a fine one to assess the fields reconstructed by the particles.

The starting point of our downscaling experience is having the large Meso-NH simulations on a 3D domain including N_c coarse cells. The time step of these simulations is denoted Δt . The particles evolve freely in the N_c cells with a time step δt , shorter than Δt . The downscaling method used in this paper involves the following four steps :

1. initializing the particles in each cell using ϵ , $\nabla_x \bar{p}$ and ΔW -velocities given by the coarse Meso-NH simulations,
2. performing particle evolution with the SLM model and the time step δt ,
3. calculating the sub-grid wind and the sub-grid turbulent parameters using the local average operator,
4. updating the values of ϵ , $\nabla_x \bar{p}$ and ΔW when the time Δt is reached, otherwise going back to step 2.

At the scale of the particles, the coarse grid-point data represent an averaged forcing. We may notice that the particle horizontal velocities are not directly forced with coarse winds. The horizontal velocities are forced with the pressure gradient and the dissipation rate. For the vertical velocities, the forcing is slightly different : it uses the vertical velocity coarse fields instead of the pressure fields. This choice has been done because horizontal velocities are driven by pressure gradients, whereas vertical velocities are driven by the buoyancy. To improve the downscaling method, temperature gradients computed from Meso-NH simulations could be taken into account. We may notice that in this work, the EDR used to force the particles is considered isotropic.

During 12 time steps, the values of the control parameters remain constant. To compute the particle simulation, the steps 2 and 3 are repeated in a continuous loop until the time Δt is reached. Then, the control parameter values are updated before computing the next 12 time steps δt (figure 4).

In this procedure, the particle management is hidden. In our simulations, the particle number is constant. In practice, we have to ensure that all the particles are in the simulation domain. In our work, the particles follow the simulated air-flow. So, at each time step some particles leave the domain. The outside particles are replaced by new particles with consistent positions and velocities as explained in section 3.3.

As the particles evolve freely in the domain, we also have to ensure a homogeneous repartition of the particles inside the domain. To do so, for each cell of the fine grid we keep the particle number between a minimal value and a maximal value which are given at the beginning of the simulation. By

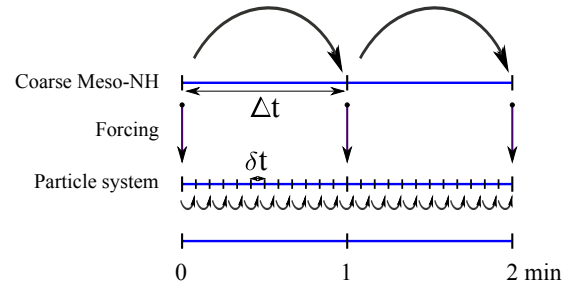


Figure 4. The different time scales used in this work. The forcing is applied at each coarse time step Δt . Between two coarse time steps, particles evolution is performed with a fine time step δt and sub-grid processes are modeled.

displacing particles, this method of particle management limits trajectory length and prevents rogue trajectories described by Yee and Wilson (2007), Postma et al. (2012), and Wilson (2013).

5 Turbulent kinetic energy

In this section we first review how TKE is computed in Meso-NH model. Then, we present the TKE computation using the particle system.

5.1 The TKE in Meso-NH

To characterize turbulence, the TKE and the EDR are the two parameters usually used. The TKE is the turbulent kinetic energy associated to the small scale turbulent structures, while the EDR quantifies the energy transfer from the large scale structures to the small scale structures.

In this work, the two turbulent parameters play different roles. The EDR is used to force the particle system, whereas the TKE is used to assess the particle representation. For the EDR fields, we use directly the Meso-NH variable. It is computed from the TKE using a closure hypothesis based on the mixing length. We give now details about how the TKE is computed.

The TKE modeled by Meso-NH is made of two terms : the resolved TKE and the sub-grid TKE. The resolved TKE is a diagnostic variable. It is calculated using the grid-point 3D wind field (u, v, w) :

$$K_{res} = \frac{1}{2} (\overline{(u - \bar{u})^2} + \overline{(v - \bar{v})^2} + \overline{(w - \bar{w})^2})$$

where the bar holds for the spatial average. Here, as the domain of simulation is very small, we choose to compute the average on all the $8 \times 8 \times 4$ grid points.

The sub-grid TKE e is a prognostic variable of Meso-NH which is computed using a parametrization (Cuxart et al., 2000). In Meso-NH, the total TKE for the cell α is given

by the sum of the sub-grid TKE and the resolved TKE :

$$K_{\alpha} = K_{res} + e_{\alpha}$$

570 where e^{α} is the sub-grid TKE for the cell α .

In the Meso-NH simulations, the grid size is fine and the resolved TKE is the major contribution to the total TKE, as expected far from the surface layer.

5.2 The TKE modeled by the particle system

The particle system is used here to model the wind inside the grid Meso-NH model. As detailed in section 3.5, using the wind modeled by the particles the total TKE is directly available. The TKE associated to the particle i is computed at each time step as follows :

$$K^i = \frac{1}{2} \langle (u^i - \langle u \rangle)^2 + (v^i - \langle v \rangle)^2 + (w^i - \langle w \rangle)^2 \rangle$$

where $\langle . \rangle$ represents the local average. For the cell α , the TKE is thus given by :

$$K_{\alpha}^i = \frac{1}{N} \sum_{i=1}^N K^i$$

575 where N is the particle number in the cell α . Therefore, the TKE computation may be adapted to the grid size, and the particle fields may be compared to coarse and fine fields. Thus by construction, the TKE modeled by the particles contains small scale contributions –sub-grid for Meso-NH– and large scale contribution –resolved by Meso-NH.
580

6 Downscaling results

In the previous sections, the downscaling algorithm has been 600 described in details. The obtained results are now presented. To assess the behavior of the particle system, we compare the 3D wind given by the particle and by Meso-NH. First results 585 on the coarse grid are shown. Then we present the comparison between the particle fields and the fine Meso-NH fields. 605 Wind power spectrum densities are then presented. Finally, results for subgrid TKE are presented. This results are presented 590 separately because the subgrid TKE is computed from the particle TKE and not directly from the wind.

6.1 3D wind results

To illustrate the results of the downscaling experience, the 595 wind results on the coarse grid and on the fine grid are illustrated for one cell and for the 3 dimensions. 615

6.1.1 On the coarse grid

To model the sub-grid fields, the particles are forced by coarse grid-point fields of pressure gradient, EDR, and mean 620 vertical velocity increment.

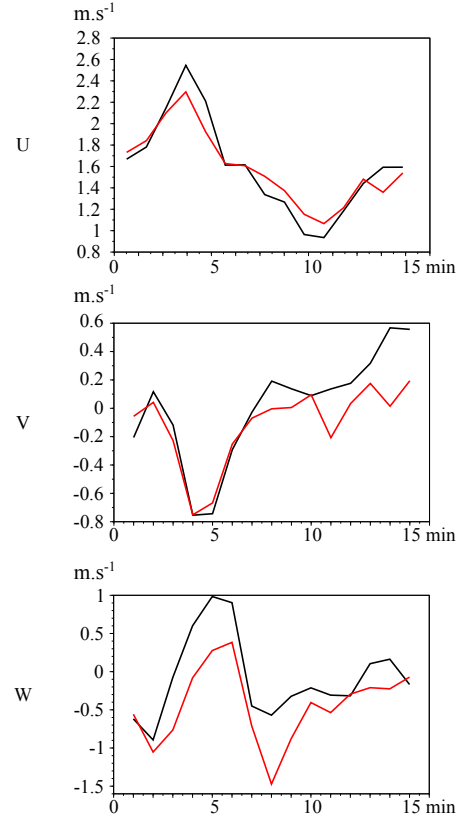


Figure 5. Time evolution of the three wind components obtained from the coarse Meso-NH simulation (black) and by the particle model (red) for one cell of the coarse grid.

To assess the downscaling method, the first thing to look at 600 is the agreement between the coarse wind and the average of the sub-grid wind modeled by the particle system. The aim is to assess the particle behaviour at the forcing scale. This verification is important, especially for the horizontal velocity 605 which is not directly forced by the coarse horizontal velocity fields. We remind that to compare the particle wind to the coarse wind fields, the particle values are averaged coarse cell by coarse cell.

Figure 5 compares the three components of the wind modeled by the particles and by Meso-NH on one cell of the coarse grid. The averaged particle wind is consistent with the coarse wind, especially for the horizontal wind. The root mean square errors associated to the first and the second particle wind components are respectively $0.045m.s^{-1}$ and $0.062m.s^{-1}$. For the vertical wind, there is more discrepancy between the particle wind and the Meso-NH wind, but they present the same variations. The associated error is $0.135m.s^{-1}$. Similar results have been obtained for the other coarse cells (not shown). Thus, as expected, the 3D wind modeled by the particles is in good agreement with the wind modeled by the coarse Meso-NH model.

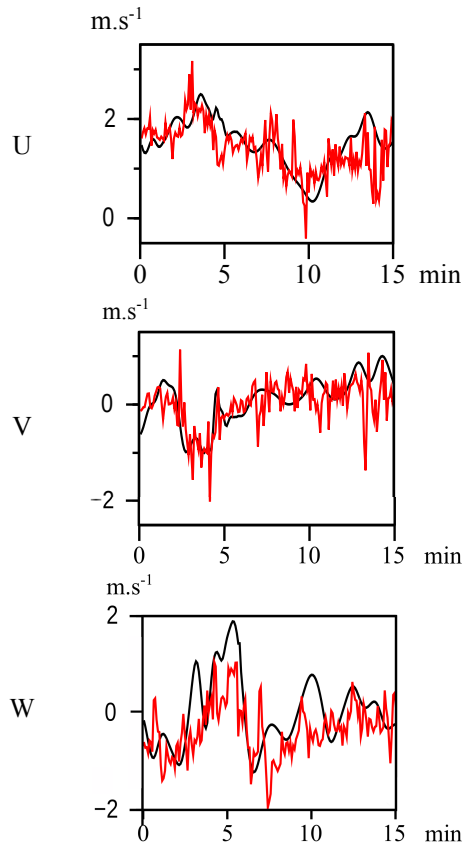


Figure 6. Time evolution of the three wind components obtained from the fine Meso-NH simulation (black) and by the particle model (red) for one cell of the fine grid.

6.1.2 On the fine grid

We are now interested in the particle behaviors at the fine scale. Here, the particle values are average fine cell by fine cell to obtain wind fields at the fine Meso-NH resolution. The particles are forced using only coarse Meso-NH fields. Thus the particle fields could differ from the reference fine Meso-NH fields.

In figure 6, the three wind components are represented for one cell of the fine grid. First, we notice the more turbulent profile of the 3D wind represented by the particles than the fine Meso-NH wind profile. Indeed, the Meso-NH wind appears smoother while the particle wind presents more temporal fluctuations. The interpretation of the power spectrum densities presented section 6.1.3 will confirm that the energy associated to high frequencies is higher in the particle wind than in the reference Meso-Nh wind.

The reference fields are represented with a 5 second time step. At this frequency, it appears that the Meso-NH wind is smoother than wind usually observed in the boundary layer. By comparison, the fluctuating profile of the particle wind

seems consistent with wind observations obtained by a 3D sonic anemometer mounted above tethered balloon (figure ??see Canut et al. (2016) for instance).

To explain the smoothness of the Meso-NH wind, two comparisons have been done. First we have compared the wind fields on the studied area to fields on different areas on the same vertical level. Subsiding or ascending areas have been chosen. It appears that Meso-NH models a smooth wind, in both ascending and subsiding areas. Then, a simulation without numerical diffusion has been performed, and the winds modeled with and without diffusion have been compared. This comparison shows that the smoothness is not due to the numerical diffusion used in the simulations.

~~Time series of the observed wind in three dimensions, from tethered balloon observations at 550m, the 06/20/2011. The wind observation frequency is 10Hz.~~

Coming back to figure 6, we can see that the particle wind seems to follow the fluctuations of the Meso-NH wind. This remark leads us to look at the low frequency component of the particle wind. In section 6.1.3, the difference between the particle wind and its low frequency component is also investigated.

To check that the particle wind follows mainly the Meso-NH wind fluctuations, we apply a low pass filter on the particle wind. The aim is to suppress the fast fluctuations and then to assess the low frequency component of the particle wind. A second order low pass filter with a cutoff frequency of $2.10^{-2}s^{-1}$ has been used.

The results are presented in figure 7. Thanks to the low pass filter we are able to compare easily the particle wind time series to the Meso-NH wind time series. The low frequency component of the particle wind presents the same variations than the reference Meso-NH wind. However one can notice that the results are better for the horizontal wind components than for the vertical one. To improve this point, one way could be to supplement the SLM with an equation for the temperature to model buoyancy effect. According to these results, the filtered particle wind seems consistent with the fine Meso-NH wind.

The particle wind fields do contain the same low frequency information than the fine Meso-NH wind fields. Thus the suggested downscaling method and the model coupling have worked. Comparing to the Meso-NH wind, the particle wind has a faster fluctuating component. The question is now to determine if the fast fluctuations are due to smaller turbulent structures than those modeled by Meso-NH or if they are only a noise added to the low frequency signal.

To propose a beginning of an answer, we present the study of the power spectrum densities (PSDs) of the wind and its low and high frequency components in section 6.1.3.

6.1.3 Validation using PSD and wind anomalies

To further the comparison between the Meso-NH wind and the particle wind, we have computed the wind PSDs. First,

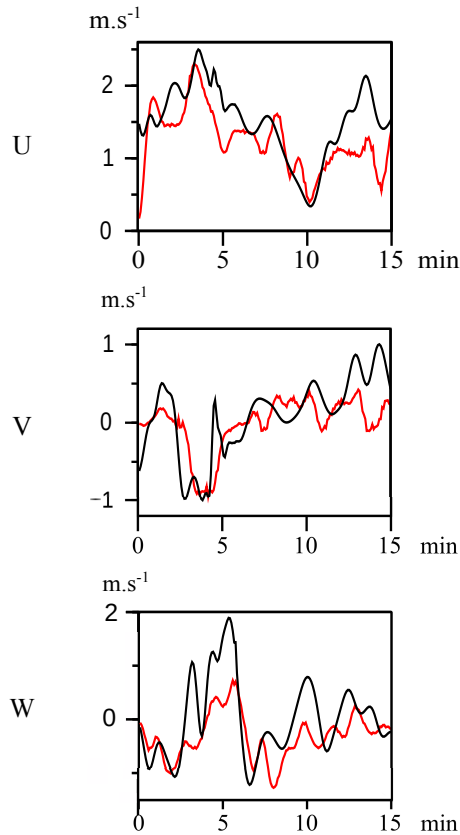


Figure 7. Components of the fine Meso-NH wind in black and components of the particle wind in red, for one cell on the second level of the fine grid.

ularity of the slope is a good point to assess the particle wind and its fast fluctuations. It shows that the energy cascades are the same whatever the considered scales. However the slope is slightly more gentle than the energy cascade. There may be too much energy associated to the turbulence modeled by the particles at high frequencies. As presented in section 3, the SLM has been designed to follow Kolmogorov [laws theory](#), but the spectra in figure 8 have been obtained by applying the model in a new framework. Our work is a first attempt to use control parameters given by an Eulerian grid point simulation. In this framework, the model behaviour has not been completely assessed yet. Longer simulations are needed to continue working on it.

Contrary to the particle wind, the Meso-NH wind spectra have a shape of spoon : they follow the $-5/3$ slope at low frequencies, then the spectrum slopes become steeper and finally the slopes are almost horizontal at high frequencies. Thus, the PSDs show that Meso-NH correctly represents the low frequency components of the wind but the modeling worsens gradually following the frequency increase. At high frequency, the Meso-NH wind PSDs look like low energetic white noises. From the spectral analysis, we may deduced an effective temporal resolution of Meso-NH about 50 seconds or $10 \cdot \delta t$. It leads that Meso-NH does not model the high frequency components of the wind. Therefore it may explain the difference between the particle wind and the Meso-NH wind we have seen in the previous section.

The spectral analysis of the time series has clarified the validity domain –in terms of temporal resolution– of the two simulations. It also shows the limit of the grid-point model for high frequency wind fluctuation modeling.

spectra of time series have been studied. Then, the PSD of the wind anomalies – differences between the particle wind and its low frequency component– are shown. Finally, we discuss briefly the effective resolution of the Meso-NH model by comparison with the LES model of the NCAR.

To assess the temporal variability of the particle wind, time PSDs are computed. For each vertical level, the PSDs are computed using groups of 4×4 fine grid cells. Each of these groups contains fine cells which are forced by a same coarse cell. A Fourier transform has been applied on time series of each fine cell. Then the Fourier coefficients of the 4×4 cells are averaged. This operation gives 4 PSDs per vertical level. The aim is to check the consistency of the different winds with the K41 [laws theory](#) (Kolmogorov, 1941).

Figure 8 presents the PSDs of the three components of the fine Meso-NH wind and of the particle wind. It appears that none of the particle wind or the fine Meso-NH wind follows perfectly the energy cascade given by the Kolomogorov's theory and represented by the $-5/3$ slope. But we may notice that the particle wind spectra present a regular slope. The reg-

The spatial resolution of the particle simulations is trickier to estimate. A first estimation may be given by the Lagrangian lengths associated to the wind components. The lengths can be evaluated using the power spectrum densities and the mean velocities. Looking at the spectrum of the first component of the wind, we can see that the spectrum is flat for frequencies higher than $5 \cdot 10^{-2} \text{s}^{-1}$ (figure 8). In average over the domain, the first component of the particle wind is about 1.3m/s. Thus a Lagrangian length associated to the particles for the first wind component is about 26m. Using the same cut-off frequency, we obtain Lagrangian lengths about 6m and 4m for the second and the third wind component respectively. The differences between the lengths computed for the three components clearly show the difficulty to use this method to evaluate the spatial resolution of the particle simulations.

To have an idea of the Meso-NH effective spatial resolution, we have compared the Meso-NH simulations to other simulations performed for the BLLAST experiment. Spatial PSDs are computed for a given time step on the whole domain – $256 \times 256 \times 256$ cells– using rows or columns of the fine grid. As for the time PSD, spatial PSD are performed using averages of Fourier coefficients. The PSDs along the x-axis

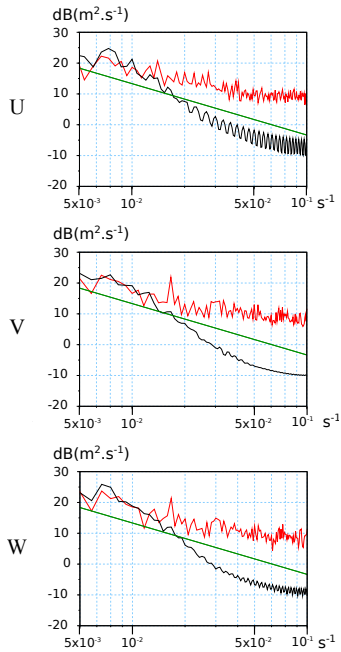


Figure 8. Power spectrum densities of the components of the fine Meso-NH wind in black and of the components of the particle wind in red, calculated on a 4x4 grid cells domain, for the second level of the fine grid. In green we have the -5/3 slope according to the K41 [lawstheory](#).

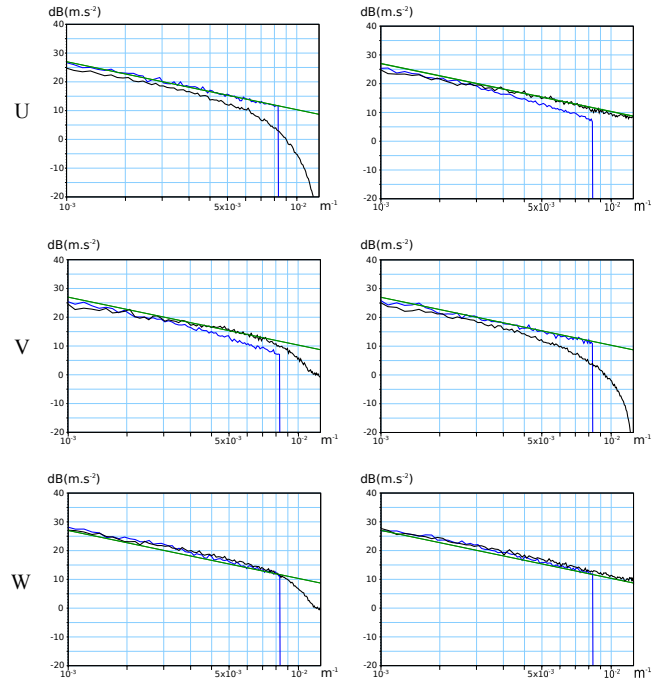


Figure 9. "Row-average" (left) and "Column-average" (right) spatial PSD on the 256x256 cells grid of the components of the wind for Meso-NH in black and the LES model of the NCAR in blue. In green we have the -5/3 slope according to the K41 [lawstheory](#).

are based on the averages of the Fourier transforms of the rows. Respectively, for the PSDs along the y-axis we use the averages of the Fourier transforms of the columns.

In this paragraph, the particle wind PSDs are not available. ⁸⁰⁰ Indeed, the downscaling experience has been performed on a restricted domain which is far too small to compute the spatial PSDs.

Thus to have a comparative element, simulations of the NCAR LES are used (Moeng, 1984). These simulations ⁸⁰⁵ have been performed by Darbieu et al. (2015). The spatial PSDs are computed for the two models using the data of the 06/20/2011 at 14h00 for the vertical level around 360 meters. Figure 9 shows the PSDs obtained for the three components of the wind following the two horizontal directions. ⁸¹⁰ The Meso-NH spectra and the NCAR LES spectra follow perfectly the energy cascade at low and medium frequencies.

At high frequencies, their shapes differ. From its formulation, the NCAR LES model spectra show a clear cutting frequency. This frequency is around $8.10^{-3}m^{-1}$. The Meso- ⁸¹⁵ NH spectra show instead gradual decreases, but the spatial resolution seems almost equivalent to the NCAR LES model. According to the NCAR LES cutting frequency, the effective spatial frequency of the Meso-NH model is about 125m. Thus it leads to an effective resolution of $3.\Delta x$, which is in ⁷⁹⁰ good agreement with previous studies (Ricard et al., 2013). ⁷⁹⁵

We may also notice the asymmetry of the spectra. It shows that the structures in the boundary layer are organized following preferential directions.

The study of the spatial spectra has shown that Meso-NH is able to model the spatial variability of the wind with a $3.\Delta x$ resolution. However Meso-NH is not able to model the local wind fluctuations under its effective resolution. Once again, it explains why the Meso-NH wind simulation is smoother than the particle simulation.

To end the validation of the particle wind, we have studied the wind anomaly PSDs. The wind anomalies are defined here as the difference between the wind and its low frequency component. The study shows that the time PSDs of the anomalies follow the energy cascade. So, the anomalies are not a white noise. Thus the particles do not add a simple noise to the coarse wind. The added information is in good agreement with the Kolmogorov K41 [lawstheory](#). It illustrates the effective working of the suggested downscaling method.

6.2 Turbulent kinetic energy results

In this section, the TKE simulated using the particle system is presented. As explained in section 4.2, the TKE is not directly forced by the coarse Meso-NH model. The particle

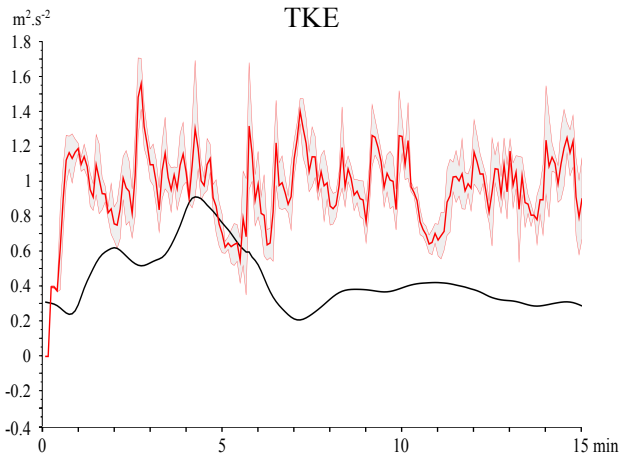


Figure 10. Fine Meso-NH TKE in black and particle TKE in red, for one cell of the fine grid. The gray zone represents the standard deviation of the particle TKE, for the particles in the cell.

TKE is computed at each fine time step δt , as it has been described in section 5. Then the particle TKE is compared to the fine Meso-NH TKE.

The results are presented in figure 10. In this figure, we focus on the same cell than the one shown in the previous sections. First, we may notice that the particle TKE is twice higher than the Meso-NH TKE. The particle system models also an important time variability for the TKE, whereas the Meso-NH TKE is rather smooth. The particle system models more small scale turbulence than Meso-NH. Thus the results for the TKE modeling are in good agreement with our previous remarks on the wind results and the Meso-NH effective time resolution.

In Lothon et al. (2014) and [Canut et al. \(2016\)](#), a study of the TKE evolution during the BLLAST experiment is presented. The authors give several observations time series of TKE. During the afternoon, TKE values are around $1 m^2 \cdot s^{-2}$, before decreasing at the end of day.

To force the particle system, we have used data from 360m and 400m high, from 13h55 UTC to 14h10 UTC. There is no TKE observation at this precise height during this period, but sonic anemometer and tethered balloon observations are available at several heights from 30m to 550m depending on the time. The TKE observations obtained using these instruments for the 06/20/2011 are given in [Canut et al. \(2016\)](#).

Comparing the particle TKE to the TKE observations, we may see that the particle TKE has the same order of magnitude than the TKE observed during the afternoon, from $0.6 m^2 \cdot s^{-2}$ to $1.7 m^2 \cdot s^{-2}$. A look at the Meso-NH TKE shows that the Meso-NH model seems to underestimate the TKE. This underestimation has already been described in previous works (Darbieu et al., 2015).

The comparison of the particle TKE with the observations shows encouraging results. These results are a first step to

demonstrate the ability of the particle system to model very small scale turbulence. However, to end the validation, the suggested downscaling method will be applied to a larger domain and to other field experiment cases.

7 Sensitivity to the forcing grid

In the previous section, all the presented results have been obtained using the same forcing scale. Here, we suggest to briefly look at the influence of the forcing scale on the fields modeled with the particle system. As a first approach to qualify this influence, the particle system has been forced by two different scales.

The previously used grid was $160m \times 160m \times 24m$ large. The new grid used to evaluate the forcing scale influence is $80m \times 80m \times 24m$ large. [This new grid is obtained by averaging the fine grid on \$2 \times 2 \times 2\$ cells.](#) The temporal resolution of the forcing is the same for the two experiences ($\Delta t = 1min$).

First the particle winds are compared to the fine Meso-NH wind. The root mean square error (RMSE) between each particle wind and the Meso-NH wind are presented in table 1. The RMSEs of the low frequency components are also presented. To compute these RMSEs, we have only used the first 5 minutes of our downscaling simulations.

Table 1. Wind RMSE depending on the forcing scale.

	160m	80m
RMSE – signal total	0.520	0.462
RMSE – signal basse fréq.	0.523	0.429

As we can expect, the particle wind obtained with the finest forcing grid is the closest to the Meso-NH wind. However, the difference between the two forcing methods are rather small. Using the finest grid reduces the RMSE of 12% for the total wind, and of 20% for the low frequency component.

The influence of the forcing scale on the TKE is illustrated in figure 11. The differences between the two forcing methods are mostly visible for the first minute of the simulation, which correspond to the first large time step. The TKE obtained with the finest forcing is closest to the forcing model TKE. This particle TKE is also less fluctuating than the TKE obtained with the largest scale forcing, but they reach the same order of magnitude.

According to these results, the two particle simulations are consistent. Reducing the forcing scale reduces the difference between the particle fields and the model fields. However, for the two forcing scales, the particle fields are more turbulent than the Meso-NH fields.

To complete the work on the sensitivity to the forcing scale, a forcing grid of $40m \times 40m \times 12m$ has also been used. The fields modeled with this forcing grid represent sub-grid fields for the fine Meso-NH simulation. As expected, the par-

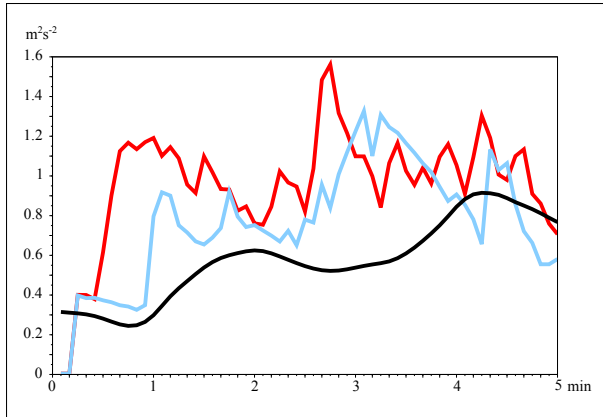


Figure 11. 5 minutes time series of TKE depending on the forcing scale : the TKE obtained with 160m x 160m x 24m is drawn in red, and the TKE obtained with 80m x 80m x 24m is drawn in blue. The fine Meso-NH TKE is drawn in black.

900 title fields are more turbulent than the fine Meso-NH fields, but they are similar to the previous sub-grid simulations (not shown).

8 Discussion

This article presents a first work on a new way to model sub-grid processes using particle systems. One of the major improvement is the use of a simple turbulence model instead of complex model such as LES or DNS. However, to fully validate the method, one of the first steps should be to use a DNS or to apply the downscaling method to a toy model to know exactly the sub-grid fields. Unfortunately, such a validation could not have been done yet.

This experience has been realized on a small domain, with a reduced number of particles in each cell. These two constraints were related to the long computational time. Extending the domain and the duration of the simulation should be one of the next steps. It would improve the PSD quality, and limit the influence of the edges. Then, a supplementary work on the spatial resolution of the particle simulations might be done and the result robustness may be tested. To give a very first answer to the robustness issue, we remind that we have compared the studied fields to fields on different areas on the same vertical level. The comparison has shown that Meso-NH fields are similar in the different areas. Thus, the downscaling method should provide similar results when being applied in these areas.

925 Related to the question of the spatial resolution of particle simulations, there is also the fundamental question of the scale of the turbulence represented in the particle fields. So far, only a first estimation of the scale has been given, and a specific work has still to be done to figure out the scales

930 represented by the particle model.

In this work, the coarse fields were computed by averaging the fine Meso-NH fields. In a more advanced experience, the coarse fields would be real Meso-NH fields computed with a coarse grid. To further this study, we could also add to the SLM an equation to model the temperature evolution. Therefore the sub-grid buoyancy effect could be modeled and compared to a high resolution Meso-NH simulation.

935 Concerning the SLM, another point has to be discussed. The Wiener processes used for the dispersion terms involve a locally Gaussian assumption of the pdf described by the particles. In our work, the Gaussian assumption is not valid at the grid cell scale. Indeed, at a given time in a given cell, particles with different characteristics are mixed. This is partially due to the free evolution of the particles in the domain. Thus the velocity pdf described by the particles in one fine cell is obtained by mixing Gaussian pdf but it is not necessarily Gaussian.

940 We would like to underline an important point about the EDR fields used to force the particle system. Here, the chosen EDR is the Meso-NH variable. The advantage of this choice is that the EDR is directly available. However, as it is a diagnostic variable of the Meso-NH model, it is computed using a closure scheme. The closure scheme may induce errors on the EDR modeling due to the underlying assumptions. To control the assumptions which are made, we could compute the EDR from the grid point wind field, and compare it to the EDR calculated using different closure schemes. As the EDR controls the particle dispersion, an improvement in the EDR modeling will directly lead to an improvement in the sub-grid turbulence modeling.

955 Therefore, among the future works, there is the application of the downscaling method to a larger domain, and the comparison of the sub-grid fields to observations. Then, there is the study of the TKE parametrization used in Meso-NH by comparison with the TKE modeled by the particles. Despite the computational time, in a long-term perspective we may also think to experiences where the sub-grid parametrization used in Meso-NH will be replaced by sub-grid particle modeling. Indeed, for research purposes, the downscaling method may be an alternative solution to common turbulence closures which often assume isotropic and homogeneous turbulence.

9 Conclusions

We present here a new downscaling method based on the coupling of a grid-point model and a particle model. The downscaling method has been applied to a simulation performed for the BLLAST experiment.

The particle system has been forced by a coarse model. Then the particle fields have been assessed against a high resolution simulation. The particle wind seems in good agree-

ment with the high resolution wind, but higher resolution simulations should be performed. The same conclusions are given for the TKE simulations.

Even if the domain size is a limitation of the present study, the presented results are very encouraging. They prove the relevance of the suggested forcing method. Forcing particle system is a quite simple process, and the sub-grid fields seem consistent with observations. Therefore, the first step to couple the SLM model and the Meso-NH model is achieved.

In a longer term, this work may be used to compare and to test the different turbulent schemes, parameterizations, or closure hypothesis available in the research models and in the operational weather forecast models.

Acknowledgements. BLLAST field experiment was made possible thanks to the contribution of several institutions and supports : INSU-CNRS (Institut National des Sciences de l'Univers, Centre national de la Recherche Scientifique, LEFE-IDAO program), Météo-France, Observatoire Midi-Pyrénées (University of Toulouse), EUFAR (EUropean Facility for Airborne Research) and COST ES0802 (European Cooperation in the field of Scientific and Technical). The field experiment would not have occurred without the contribution of all participating European and American research groups, which all have contributed in a significant amount. BLLAST field experiment was hosted by the instrumented site of Centre de Recherches Atmosphériques, Lannemezan, France (Observatoire Midi-Pyrénées, Laboratoire d'Aérodynamique). The 60m tower is partly supported by the POCTEFA/FLUXPYR European program. BLLAST data are managed by SEDOO, from Observatoire Midi-Pyrénées. The French ANR (Agence Nationale de la Recherche) supports BLLAST analysis in the 2013-2015 BLLAST_A project. The authors also thank Clara Dardieu for providing the NCAR LES simulations, and Bruno Pignatelli for the tethered balloon observations.

References

- Andrews, N. F.: Simulating the diurnal cycle of the atmospheric boundary layer using large-eddy simulation with vertical adaptive mesh refinement, Ph.D. thesis, The University of Utah, 2012.
- Baehr, C.: STOCHASTIC MODELING AND FILTERING OF DISCRETE MEASUREMENTS FOR A TURBULENT FIELD. APPLICATION TO MEASUREMENTS OF ATMOSPHERIC WIND, *International Journal of Modern Physics B*, 23, 5424–5433, 2009.
- Baehr, C.: Nonlinear filtering for observations on a random vector field along a random path. Application to atmospheric turbulent velocities, *ESAIM: Mathematical Modelling and Numerical Analysis*, 44, 921–945, 2010.
- Bally, V. and Talay, D.: The law of the Euler scheme for stochastic differential equations, *Probability theory and related fields*, 104, 43–60, 1996.
- Bernardin, F., Bossy, M., Chauvin, C., Drobinski, P., Rousseau, A., and Salameh, T.: Stochastic downscaling method: application to wind refinement, *Stochastic Environmental Research and Risk Assessment*, 23, 851–859, 2009.
- Bernardin, F., Bossy, M., Chauvin, C., Jabir, J.-F., and Rousseau, A.: Stochastic Lagrangian method for downscaling problems in computational fluid dynamics, *ESAIM: Mathematical Modelling and Numerical Analysis*, 44, 885–920, 2010.
- Blayo, E. and Debreu, L.: Adaptive mesh refinement for finite-difference ocean models: first experiments, *Journal of Physical Oceanography*, 29, 1239–1250, 1999.
- Bogenschütz, P. A. and Krueger, S. K.: A simplified PDF parameterization of subgrid-scale clouds and turbulence for cloud-resolving models, *Journal of Advances in Modeling Earth Systems*, 5, 195–211, 2013.
- Brackbill, J. U., Kothe, D. B., and Ruppel, H. M.: FLIP: A low-dissipation, particle-in-cell method for fluid flow, *Computer Physics Communications*, 48, 25–38, 1988.
- Canut, G., Couvreur, F., Lothon, M., Legain, D., Pignatelli, B., Lampert, A., Maurel, W., and Moulin, E.: Turbulence fluxes and variances measured with a sonic anemometer mounted on a tethered balloon, *Atmospheric Measurement Techniques*, 9, 4375–4386, 2016.
- Colella, P. and Woodward, P. R.: The piecewise parabolic method (PPM) for gas-dynamical simulations, *Journal of computational physics*, 54, 174–201, 1984.
- Couvreur, F., Guichard, F., Redelsperger, J., Kiemle, C., Masson, V., Lafore, J., and Flamant, C.: Water-vapour variability within a convective boundary-layer assessed by large-eddy simulations and IHOP_2002 observations, *Quarterly Journal of the Royal Meteorological Society*, 131, 2665–2693, 2005.
- Cuxart, J., Bougeault, P., and Redelsperger, J.-L.: A turbulence scheme allowing for mesoscale and large-eddy simulations, *Quarterly Journal of the Royal Meteorological Society*, 126, 1–30, 2000.
- Dardieu, C., Lohou, F., Couvreur, F., Lothon, M., Durand, P., Guichard, F., and Patton, N.: 7B. 1 Large eddy simulations of convective boundary layer during late afternoon transition, *Symposium on Boundary Layers and Turbulence*, Boston, 2012.
- Dardieu, C., Lohou, F., Lothon, M., Vilà-Guerau de Arellano, J., Couvreur, F., Durand, P., Pino, D., G Patton, E., Nilsson, E., Blay-Carreras, E., et al.: Turbulence vertical structure of the boundary layer during the afternoon transition, *Atmospheric Chemistry and Physics*, 15, 10 071–10 086, 2015.
- Debreu, L., Blayo, E., and Barnier, B.: A general adaptive multi-resolution approach to ocean modelling: Experiments in a primitive equation model of the North Atlantic, in: *Adaptive Mesh Refinement-Theory and Applications*, pp. 303–313, Springer, 2005.
- Drobinski, P., Steinacker, R., Richner, H., Baumann-Stanzer, K., Beffrey, G., Benech, B., Berger, H., Chimani, B., Dabas, A., Dorninger, M., et al.: Föhn in the Rhine Valley during MAP: A review of its multiscale dynamics in complex valley geometry, *Quarterly Journal of the Royal Meteorological Society*, 133, 897–916, 2007.
- Durbin, P.: A stochastic model of two-particle dispersion and concentration fluctuations in homogeneous turbulence, *Journal of Fluid Mechanics*, 100, 279–302, 1980.
- Durrán, D. R.: Improving the anelastic approximation, *Journal of the atmospheric sciences*, 46, 1453–1461, 1989.
- Hagelin, S., Auger, L., Brovelli, P., and Dupont, O.: Nowcasting with the AROME model: First results from the high-resolution AROME Airport, *Weather and Forecasting*, 29, 773–787, 2014.

- Honnert, R., Masson, V., and Couvreur, F.: A diagnostic for evaluating the representation of turbulence in atmospheric models at the kilometeric scale, *Journal of the Atmospheric Sciences*, 68, 3112–3131, 2011.
- Jam, A., Hourdin, F., Rio, C., and Couvreur, F.: Resolved versus parametrized boundary-layer plumes. Part III: Derivation of a statistical scheme for cumulus clouds, *Boundary-layer meteorology*, 147, 421–441, 2013.
- Jimenez, M. A., Angevine, W. M., Bazile, E., Couvreur, F., Cuxart, J., Pino, D., and Sastre, M.: An intercomparison of mesoscale simulations during the Boundary Layer Late Afternoon and Sunset Turbulence (BLLAST) experimental field campaign, in: EGU General Assembly Conference Abstracts, vol. 16, p. 1629, 2014.
- Kolmogorov, A.: The local structure of turbulence in incompressible viscous fluid for very large Reynolds' numbers, in: *Akademiia Nauk SSSR Doklady*, vol. 30, pp. 301–305, 1941.
- Lafore, J. P., Stein, J., Asencio, N., Bougeault, P., Ducrocq, V., Duron, J., Fischer, C., Hérelil, P., Mascart, P., Masson, V., et al.: The Meso-NH atmospheric simulation system. Part I: adiabatic formulation and control simulations, in: *Annales Geophysicae*, vol. 16, pp. 90–109, Springer, 1998.
- Larson, V. E., Golaz, J.-C., and Cotton, W. R.: Small-scale and mesoscale variability in cloudy boundary layers: Joint probability density functions, *Journal of the atmospheric sciences*, 59, 3519–3539, 2002.
- Larson, V. E., Schanen, D. P., Wang, M., Ovchinnikov, M., and Ghan, S.: PDF parameterization of boundary layer clouds in models with horizontal grid spacings from 2 to 16 km, *Monthly Weather Review*, 140, 285–306, 2012.
- Lothon, M., Lohou, F., Pino, D., Couvreur, F., Pardyjak, E., Reuder, J., Vilà-Guerau de Arellano, J., Durand, P., Hartogensis, O., Legain, D., et al.: The BLLAST field experiment: Boundary-layer late afternoon and sunset turbulence, *Atmospheric Chemistry and Physics*, 14, 10 931–10 960, 2014.
- Machado, L. A. and Chaboureau, J.-P.: Effect of Turbulence Parameterization on Assessment of Cloud Organization, 2014.
- Moeng, C.-H.: A large-eddy-simulation model for the study of planetary boundary-layer turbulence, *Journal of the Atmospheric Sciences*, 41, 2052–2062, 1984.
- Nilsson, E., Lohou, F., Lothon, M., Pardyjak, E., Mahrt, L., and Darbieu, C.: Turbulence Kinetic Energy budget during the afternoon transition—Part 1: Observed surface TKE budget and boundary layer description for 10 intensive observation period days, *Atmospheric Chemistry and Physics*, 15, 29 747–29 805, 2016.
- Nyquist, H.: Certain Factors Affecting Telegraph Speed, *Bell System technical journal*, 3, 324–346, 1924.
- Nyquist, H.: Certain topics in telegraph transmission theory, 1928.
- Pardyjak, E., Alexander, D., Lothon, M., Lohou, F., Derrien, S., Reuder, J., Darbieu-Biasini, C., Legain, D., Traullé, O., de Coster, O., et al.: First results from the surface heterogeneity focus area of the Boundary Layer Late Afternoon and Sunset Turbulence (BLLAST) Experiment, in: *AGU Fall Meeting Abstracts*, vol. 1, p. 0034, 2011.
- Perraud, E., Couvreur, F., Malardel, S., Lac, C., Masson, V., and Thouron, O.: Evaluation of statistical distributions for the parametrization of subgrid boundary-layer clouds, *Boundary-layer meteorology*, 140, 263–294, 2011.
- Pope, S.: Lagrangian PDF methods for turbulent flows, *Annual review of fluid mechanics*, 26, 23–63, 1994.
- Pope, S. B.: *Turbulent flows*, Cambridge university press, 2000.
- Postma, J. V., Yee, E., and Wilson, J. D.: First-order inconsistencies caused by rogue trajectories, *Boundary-layer meteorology*, 144, 431–439, 2012.
- Redelsperger, J.-L., Mahé, F., and Carlotti, P.: A simple and general subgrid model suitable both for surface layer and free-stream turbulence, *Boundary-layer meteorology*, 101, 375–408, 2001.
- Ricard, D., Lac, C., Riette, S., Legrand, R., and Mary, A.: Kinetic energy spectra characteristics of two convection-permitting limited-area models AROME and Meso-NH, *Quarterly Journal of the Royal Meteorological Society*, 139, 1327–1341, 2013.
- Rotach, M., Andretta, M., Calanca, P., Weigel, A., and Weiss, A.: Boundary layer characteristics and turbulent exchange mechanisms in highly complex terrain, *Acta Geophysica*, 56, 194–219, 2008.
- Rotach, M. W., Calanca, P., Graziani, G., Gurtz, J., Steyn, D. G., Vogt, R., Andretta, M., Christen, A., Cieslik, S., Connolly, R., et al.: Turbulence Structure and Exchange Processes in an Alpine Valley: The Riviera Project., 2004.
- Rousseau, A., Bernardin, F., Bossy, M., Salameh, T., and Drobniski, P.: Stochastic particle method applied to local wind simulation, in: *ICCEP'07-International Conference for Clean Electrical Power*, pp. 526–528, 2007.
- Sommeria, G. and Deardorff, J.: Subgrid-scale condensation in models of nonprecipitating clouds, *Journal of the Atmospheric Sciences*, 34, 344–355, 1977.
- Stohl, A. and Thomson, D. J.: A density correction for Lagrangian particle dispersion models, *Boundary-Layer Meteorology*, 90, 155–167, 1999.
- Thomson, D.: Criteria for the selection of stochastic models of particle trajectories in turbulent flows, *Journal of Fluid Mechanics*, 180, 529–556, 1987.
- Thomson, D.: A stochastic model for the motion of particle pairs in isotropic high-Reynolds-number turbulence, and its application to the problem of concentration variance, *Journal of Fluid Mechanics*, 210, 113–153, 1990.
- Uliasz, M.: Lagrangian particle dispersion modeling in mesoscale applications, *SMR*, 760, 23, 1994.
- Wilson, J. D.: “Rogue Velocities” in a Lagrangian Stochastic Model for Idealized Inhomogeneous Turbulence, *Lagrangian Modeling of the Atmosphere*, pp. 53–58, 2013.
- Yee, E. and Wilson, J. D.: Instability in Lagrangian stochastic trajectory models, and a method for its cure, *Boundary-layer meteorology*, 122, 243–261, 2007.